24th COBEM - 2017

24th ABCM International Congress of Mechanical Engineering
December 3-8, 2017, Curitiba, PR, Brazil

COBEM-2017-2690
CHARACTERIZATION OF NITINOL ALLOY IN THE COMMERCIAL STATE

Rivaldo Lins [*a]
José Augusto [a]
[a] DEMAT, CT, UFRN, Av. Sen. Salgado Filho, 3000, CEP 59072-970 Natal, RN, Brazil
buschinelli@ct.ufrn.br

Ricardo Alves [b]
[b] DEM, CT, UFPB, Cidade Universitária, s/n - Castelo Branco III, CEP 58051-085 João Pessoa, PB, Brazil
ricardo_alves_francisco@hotmail.com

Nicolau Apoena [a]
nicolau.castro.ufrn@gmail.com

Luan Costa [a]
luanmayk.ufrn@gmail.com

Guilherme Oliveira [a]
oliveiraguilhermeg@gmail.com

Thomas Monteiro [a]
thomas.3008@outlook.com

Thiago Souza [a]
thiagos874@gmail.com

Abstract. *Shape memory alloys (SMA) are classified as active and intelligent materials. The nickel titanium (NiTi) alloy with composition around 55% by weight, better known commercially as Nitinol, corresponds to this group of metallic materials that have the ability to return to a format or size previously defined when subjected to a thermal cycle Appropriate, called "Shape Memory Effect" (SME). The phase transformation temperatures are defined as As (austenite start), Af (austenite finished), Ms (martensite start) and Mf (martensite finished), ie, beginning and end of austenitic transformation and beginning and end of martensitic transformation. The objective of the present work is the study of the NiTi alloy in relation to SME and the comparison of mechanical properties and structures by means of metallographic analyzes (optical and electron microscopy), SEM, XDR and Vickers microhardness tests under the conditions.*

Acknowledgements: *Shape Memory Alloy, Nitinol, Shape Memory Effect.*

1. INTRODUCTION

The shape memory alloys are metal alloys that have a return ability of shape or size when subjected to a heat treatment. The martensitic phase transformation promotes a shape recovery with shape memory, pseudo-elasticity, and shape memory effect. These desperate properties interest technology, and how leagues look for applications(Oliveira *et al.* 2015; Villarinho and Mecânico 2010).

It is made up of the literature that was the metallurgical researcher William F. Buehler, naval artillery laboratory of the American Navy that developed a metallic alloy with the shape memory of composition around a match of nickel and titanium in 1965, hence the acronym Nitinol (César *et al.*, 2009).

Although a variety of alloys exhibit a shape memory effect, only those that can recover a substantial deformation substance, or generate a significant force of restitution on shape shifting, commercial products.

Therefore, based on technological information, the objective of this work is to support the product designer in Nitinol, the first step is to characterize the material to be used.

2. NITINOL

Shape Memory Alloy (SMA) is part of a group of metallic materials that have the ability to recover a shape or size previously determined when subjected to an appropriate thermomechanical treatment. Metallic materials generally have a recoverable deformation of about 0.2%, while SMA materials reach 8% (Duerig and Pelton *et al.,* 1994).

2.1 SHAPE MEMORY ALLOY

It is common for these alloys to contain an excess of nickel (Ni) which may amount to about 1%. Other elements such as iron (Fe) and chromium (Cr) are also frequently added (to lower processing temperatures), as well as copper (Cu), to reduce the thermal transformation hysteresis and decrease the martensite. The presence of contaminants such as oxygen (O) and carbon (C) can also alter the transformation temperature and degrade the mechanical properties, which makes it desirable to minimize the presence of these elements (José, Silva and Grande *et al.,* 2009; Villarinho and Mecânico *et al.,* 2010).

2.2 STRUCTURES AND PROPERTIES

For the NiTi SMA the high temperature phase is the austenite (B2) with cubic structure of the centered body (CCC), which when cooled becomes monoclinic martensite (B19 'The martensite can be obtained in a single transformation step B2 → B19 'or in two transformation stages B2 → R → B19' in this case we obtain the phase R, which presents trigonal structure with angle α from the cubic cell B2, by stretching following one of the four directions <111>, it can be said that the triclinic distortion increases with the decrease of the temperature, being this effect more accentuated for NiTi rich in Ni (Otsuka *et al*., 1999). Table 1 shows the main properties of NiTi SMA.

Table 1: NiTi proprieties.

Proprieties	Austenite (B2)	Martensite (B19')
Electrical resistivity, Ω.m	$10{,}0x10^{-7}$	$8{,}0x10^{-7}$
Thermal conductivity, W / (m.K)	18,0	8,6
Magnetic susceptibility, H / (m.kg)	$4{,}8x10^{3}$	$3{,}1x10^{3}$
Expansion coefficient, K-1	$11{,}0x10^{-6}$	$6{,}6x10^{-6}$
Specific heat, J / (kg.K)	$3{,}2x10^{2}$	
Latent heat of transformation, J / kg	$2{,}4x10^{4}$	

2.3 SUPERELASTIC AND SHAPE MEMORY EFFECT

Not all the alloys that have the SME necessarily present the SE. Within the family of commercially available NiTi or nitinol alloys, some terms may be termed "pseudoplastic", "linear elastic", "non-superelastic" or "stable martensite" which, although may be similar in conventional chemistry to memory and superelastic varieties, may exhibit distinct and useful mechanical properties (Willard *et al.*, 2013). NiTi superelastic products differ from non-superelastic products in the degree of cold work produced by the manufacturing process (Thayer *et al.,* 1995).

The pseudoplastic NiTi can still accept up to about 2-5% tension while remaining in the elastic regime (does not remain with the same constancy of a superelastic alloy), which is still very good compared to ordinary steels which accepts up to about 0.44% stress before deformation plastically (irreversible), while superelastic NiTi can accept up to about 8% of strain before plastic deformation (Willard *et al.*, 2013).

Table 2: SMA temperature and efects.

Alloys	Effects	Description
Alloy N	Superelasticit	-10ºC < A_f < -15ºC
Alloy S	Superelasticit	A_f = 0ºC, more ductile than the alloy N
Alloy C	Superelasticit	Alloy with Cr, more rigid than S e N, -10ºC < A_f < -20ºC
Alloy B	Memory effect	25ºC < A_f < 45ºC
Alloy M	Memory effect	75ºC < A_f < 85ºC
Alloy H	Memory effect	95ºC < A_f < 110ºC

2.4 MANUFACTURING PROCESSES

The manufacturing process of the Nitinol alloy basically consists of five stages: fusion / casting; forging / hot rolling; cold work; conformation to the final shape and heat treatment to obtain the shape memory effect or superelasticity (Sashihara *et al.*, 2007). Such steps can be seen from the flowchart below.

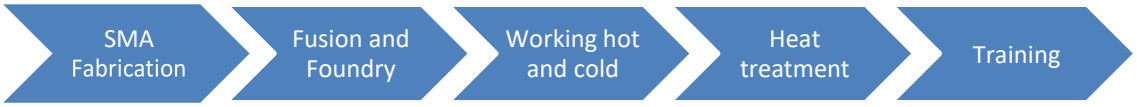

Figure 1: Stages of the manufacturing process.

The presence of oxygen promotes the formation of an inclusion of $Ti_4Ni_2O_x$ which tends to reduce the amount of titanium in the matrix. As effect, Ms becomes lower and there is retardation in grain growth (Souza *et al.*, 2017).

2.4.1 TRAINING

It is the simplest form of form memory because it requires less processing, reducing its cost (José R. Santiago Anadón *et al.*, 2002). Materials with the unidirectional memory effect feature can only resemble their original shape by applying heat to their deformed shape. The shape change occurs by means of a phase transformation, where the lattice structure, inherent to its martensitic phase, becomes an austenitic structure (Victoria and Pons *et al.*,2011).
In terms of application, intrinsic bidirectional memory effect alloys are not widespread. This is due to a greater training complexity, which involves a large number of cycles and a smaller capacity to perform the work, when compared to a memory effect unidirectional alloy (Souza *et al.*, 2017).

3. MATERIALS AND METODS

Two pieces made of NiTi from different manufacturers were analyzed and passed through different types of forming processes.

To characterize these materials, the following microstructural analyzes were done: SEM, EDS, XRD. Microhardness tests were performed for mechanical characterization.

4. EXPERIMENTAL PROCEDURE

(1) A 0.5 mm nitinol plate and a 2 mm diameter nitinol wire passed through ports for analysis. The cuts were made with a copper-coated disc with fine diamond cut, along with a Buehler IsoMet1000, Precision Salt Machine. With the following parameters: Speed of 250 rpm. Use of water-soluble refrigerant.

(2) For inlay, an Arotec PRESOM modeling machine was used, a load used of 200 Pa of pressure, maintained for 10 minutes. The pieces were embedded in conductive copper bakelite.

(3) In the sanding step, as a sheet received as a lesson and a polishing, a surface treatment and a polishing for removal of oxides and burrs. A P1200 water sandpaper was used with the machine aid: Buehler Metasevv 250 Grinder - Polisher. With the following parameters: Initial force of 25N - 30N, for a time of 3 minutes, inverted rotation with respect to the movement of sandpaper disc, with constant application of water keeping a thin film between an example and a sandpaper.

(4) In the polishing step, 2 polishing cloths were used, one of 3μm granulometry and another 1μm. With the auxiliary of the machine: Buehler Metasevv 250 Grinder - Polisher, with the following parameters: 45N-50N force for a time of 3 minutes, and application of fluids: Buehler MetaDi Supreme, Polyerystalline diamond suspension; 3μm other than 1μm (+ metal lubricant) for each cloth. To finish this stage, a final chemical abrasive treatment was carried out in another equipment, with the following parameters: 15N load keep for 1,5h, with a speed of 15 rpm. 0.02 micro ultrafine colloidal silica fluid. Remember to clean each step like pieces with cotton and detergent.

(5) Drying: keep submerged samples in Absolute 99.5 °GL ethyl alcohol in the UltraCleaner 1650 unique machine for 5 minutes leave in the Ultrasonic Cleaner, dry thoroughly and finally keep in a desiccator for microscopic analysis.

(6) A chemical solution was prepared with 81.08% acetic acid (CH_3COOH), 13.5% nitric acid (H_2NO_3), and 5.4% hydrofluoric acid (HF), leaving the sample immersed for approximately 10 seconds.

5. RESULTS AND DISCUSSION

Samples were submitted to characterization analyzes. For comparative purposes the samples were examined by field emission scanning electron microscopy (SEM-FEG), X-ray diffraction (XRD). The determination of the chemical composition was by means of EDS. Microhardness tests were performed on the material as received in the crushed state.

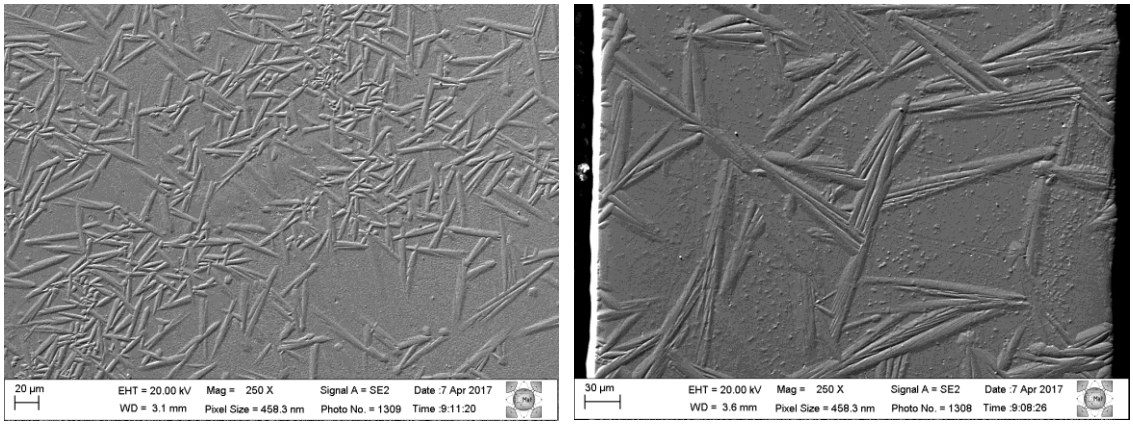

Figure 2: Nitinol plate. (A) Parallel to Support. (B) Longitudinal (cut).

Microstructural characterization techniques, via MEV-FEG (ZEISS AURIGA 40), structural characterizations via DR-X (Shimadzu LABX 7000) were used. to identify the chemical composition via EDS coupled to the SEM.

Figures 2 (a) and (b) correspond to the images obtained by SEM of the nitinol plate in commercial state, in the transverse and longitudinal direction respectively. Fig.2 (a) shows that the material is predominantly martensite phase, notable for the large amount of martensite needle throughout the sample. Apparently Fig.2 (b) appears to be with a larger application; however the two images have similar parameters, meaning the preferred direction of the structure due to processing.

Figure 3 shows the commercially available nitinol wire, for Fig. 3 (a) the wire in the longitudinal section and in Fig. 3 (b) the cross-section.

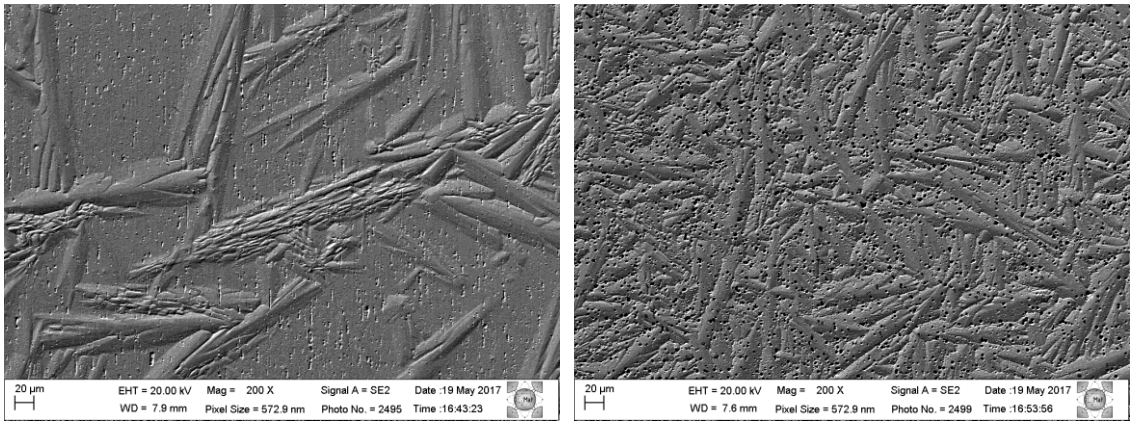

Figure 3: Longitudinal nitinol wire (a), Transverse (b).

In agreement with Fig. 3, it can be seen that, unlike the plate, the most preferred section is martensite in the transverse direction (Fig. 3a), due to the type of processing to which the material was subjected, tensile stresses than those of compression while in the laminating process more compression efforts are exerted than traction. Another characteristic perceptible is the large amount of traces and dark spots identified as precipitates which were plucked during the chemical attack. In Figure 4 we have the comparison of the two samples with 500x magnified images.

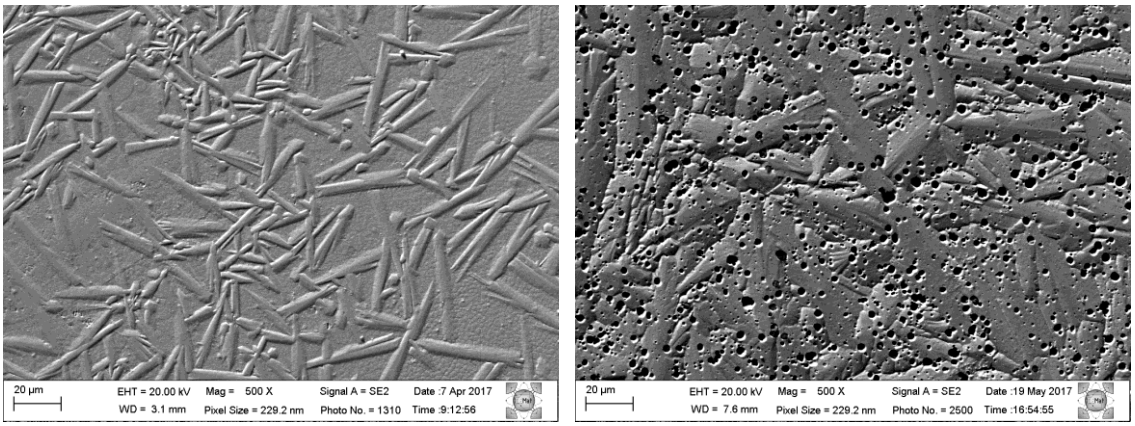

Figure 4: Nitinol plate (a) and wire (b)

According to the images obtained by the SEM the plate presents a more refined martensite compared to the wire.

Through EDS we can verify the chemical analysis of these materials and a particular region. Figure 5 shows sheet EDS.

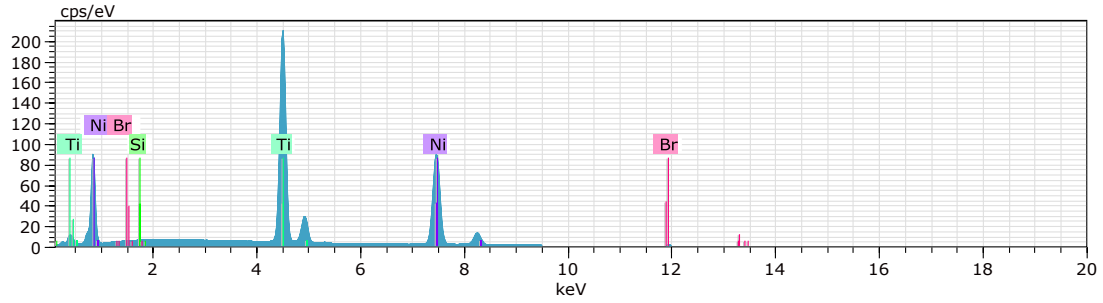

Figura 5: EDS chapa de nitinol.

In the chemical composition obtained by EDS we see the predominance of nickel and titanium with the highest energy peaks and a small peak identified as bromine (Br). In Table 3 we have the percentage at the atomic level of this material.

Composition	at.%
Ti	54,66
Ni	43,35
Br	1,85
Others	0,14
Total	**100**

Table 3: Chemical composition of nitinol sheet

Tab.3 confirms a small amount of bromine contained in the material, usually added in order to reduce the transformation temperature. Figure 5 shows the EDS graph of the nitinol wire.

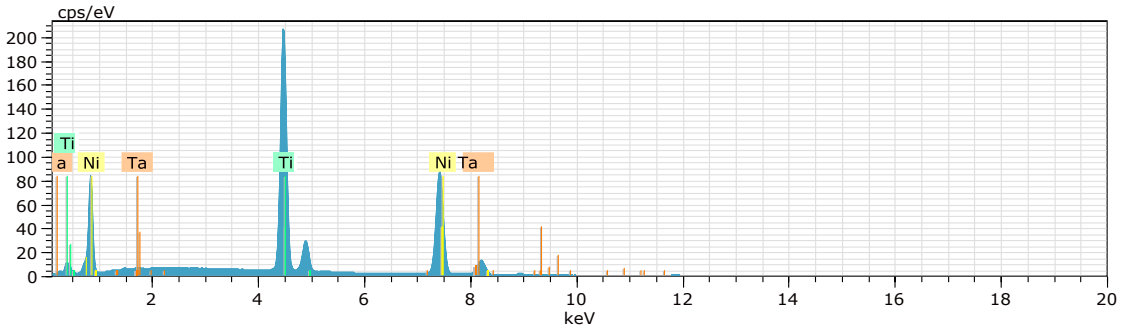

Figure 6: EDS nitinol wire.

The graph for the wire showed higher intensity for titanium and nickel as expected and a small amount of tantalum (Ta). According to Table 4 we see the percentage at atomic level of a given region.

EDS NiTi wire	at.%
Ti	54,22
Ni	43,16
Ta	2,62
Others	0
Total	**100**

Table 6: Chemical composition of nitinol wire.

Different from the plate in the wire presented a small percentage of tantalo in the material, this element is also added to control the transformation temperature.

In the graphs obtained through the XDR technique it is possible to confirm the phases present in these materials, as we can see in Figure 7.

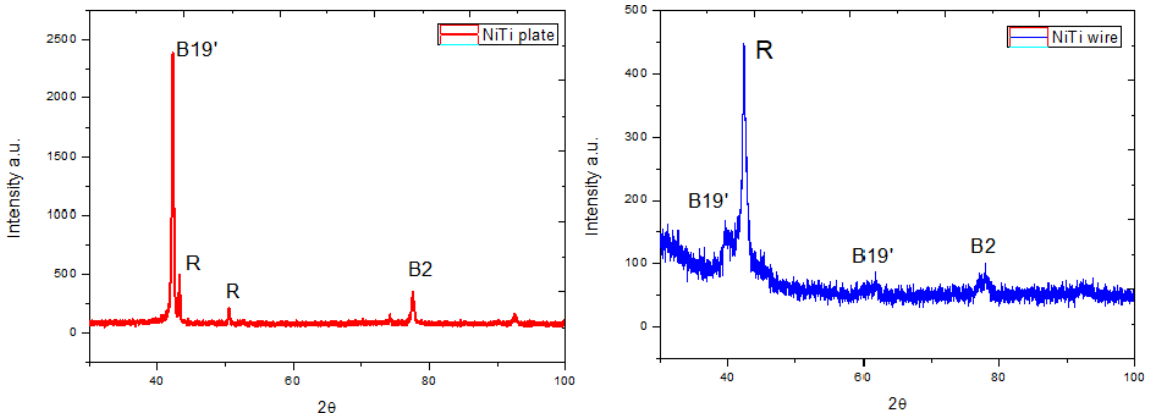

Figura 7: XDR plate (a), wire(b).

The graphs obtained by the XRD analyzes show the phases present in these materials. For the plate the main peak is characteristic of the martensitic phase B19 ', also showing some peaks identified as phase R and austenite B2 present in smaller scale. For the sample of the wire, we have the peak of greater intensity characteristic for the phase R, containing greater amount of martensite B19 'and a lower characteristic peak of austenitic phase B2 (Magela *et., al* 2010). Despite the similarity of the XRD analysis, the appearance appears to have appeared due to the type of mechanical conformation to which each material was submitted.

The Vickers microhardness measurements (MHV) were performed in the FUTURE - TECH microdurometer, model FM - 810, in Tables 7 we have the measurements.

Microhardness	Plate(MHV)	Wire(MHV)
Measures	308,6	272,1
	300,7	263,8
	294,2	297
	297,7	237,3
	313,6	292,4
	309,1	273,2
	303,5	233
	303,2	266,1
Average	**303,825**	**266,8625**

Table 7: Vickers microhardness values for nitinol sheet and wire.

In agreement with the values of microhardness obtained, it is observed that the plate is more resisistente than the wire, totaling in a value close to 300MHV, from this value the material made of nitinol presents the mechanical behavior of superelastic while the wire has effect shape memory when thermally indented.

6. CONCLUSION

It is concluded that the materials analyzed have stencils and similar compositions, but with small details determining the final functions of each, as processing techniques and different addition elements in the chemical composition. The sheet has a more refined martensite than the wire, consequently having greater strength.

7. ACKNOWLEDGEMENTS

Thanks to the Department of Materials Engineering (DeMat) of the Federal University of Rio Grande do Norte (UFRN), for the availability of sophisticated laboratories and equipment. Thanks to CAPES for student support.

8. REFERENCES

César A.B.G. 2009. *Estudo do efeito de memória de forma de fios ortodônticos da liga Ni-Ti nas condições comercial e após tratamentos térmicos* . PUCRS; Dissertation, Porto Alegre, Brazil.

Duerig, Tw W, and Ar R Pelton. 1994. *Ti-Ni Shape Memory Alloys*. Materials properties handbook: Titanium alloys 683: 1035–48.

José, Niédson, Da Silva. 2009. *Estudo do comportamento termomecânico de uma liga Ni-Ti com memória de forma usando análise dinâmico-mecânica (DMA)*.Dissertation, UFCG, Campina Grande, Brazil.

José R. Santiago Anadón. 2002. *Large Force Shape Memory Alloy Linear Actuator*. Journal of Chemical Information and Modeling 53: 1689–99.

Magela, Jardel Oliveira. 2010. *Influência de tratamentos térmicos e mecânicos nas temperaturas de transformação martensítica em ligas Ni-Ti com efeito memória de forma.* Dissertation, UEMG, Brazil.

Oliveira, Thomas S et al. 2015. *Confection and Assessment of a Dynamic Orthotics Using a Nitinol Alloy.* 5(6): 434–39.

Otsuka, Kazuhiro, and Xiaobing Ren. 1999. *Recent Developments in the Research of Shape Memory Alloys.* 7: 511–28.

Sashihara, Eduardo Massao. 2007. *Produção da liga Ni-Ti com efeito de memória de forma em forno de fusão por feixe eletrônico e sua caracterização.* Dissertation, ITA, SP, Brazil.

Souza, T. V. 2017. *Influência de tratamentos térmicos de recozimento na microestrutura de uma liga NiTi pseudoplástica.* Dissertation, UFRN, Brazil.

Thayer, Todd A., Michael D. Bagby, Robert N. Moore, and Robert J. DeAngelis. "American Journal of Orthodontics and Dentofacial Orthopedics" 1995. *X-Ray Diffraction of Nitinol Orthodontic Arch Wires*. 107(6): 604–12.

Victoria, Cristina, and Urbina Pons. 2011. *Improvement of the one-way and two-way shape memory effects in Ti-Ni shape memory alloys by thermomechanical treatments.* Thesis PhD, Universitat Rovira I Virgili, Tarragona, Spain.

Villarinho, Denis Jardim 2010. *Caracterização de Uma Liga NiTi Visando Confecção E Aplicação Como Material Biomédico Em Órtese Grampo de Judet.* Dissertation, UFRGS, Brazil.

Willard, Martin R. 2013. Patent Application Publication. *Renal nerve modulation devices and methods for renal nerve modulation*. US 20130172880A1.

9. RESPONSIBILITY NOTICE

The author(s) is (are) the only responsible for the printed material included in this paper.